Citation: Cell Death and Disease (2012) 3, e349; doi:10.1038/cddis.2012.89

www.nature.com/cddis

Glucocorticoid-mediated BIM induction and apoptosis are regulated by Runx2 and c-Jun in leukemia cells

N Heidari[1], AV Miller[2], MA Hicks[1,2], CB Marking[1] and H Harada*[,1,2]

Glucocorticoids (GCs) are common components of many chemotherapeutic regimens for lymphoid malignancies. GC-induced apoptosis involves an intrinsic mitochondria-dependent pathway. BIM (BCL-2-interacting mediator of cell death), a BCL-2 homology 3-only pro-apoptotic protein, is upregulated by dexamethasone (Dex) treatment in acute lymphoblastic leukemia cells and has an essential role in Dex-induced apoptosis. It has been indicated that Dex-induced BIM is regulated mainly by transcription, however, the molecular mechanisms including responsible transcription factors are unclear. In this study, we found that Dex treatment induced transcription factor Runx2 and c-Jun in parallel with BIM induction. Dex-induced BIM and apoptosis were decreased in cells harboring dominant-negative c-Jun and were increased in cells with c-Jun overexpression. Cells harboring short hairpin RNA for Runx2 also decreased BIM induction and apoptosis. On the *Bim* promoter, c-Jun bound to and activated the AP-1-binding site at about −2.7 kb from the transcription start site. Treatment with RU486, a GC receptor antagonist, blocked Dex-induced Runx2, c-Jun and BIM induction, as well as apoptosis. Furthermore, pretreatment with SB203580, a p38-mitogen-activated protein kinase (MAPK) inhibitor, decreased Dex-induced Runx2, c-Jun and BIM, suggesting that p38-MAPK activation is upstream of the induction of these molecules. In conclusion, we identified the critical signaling pathway for GC-induced apoptosis, and targeting these molecules may be an alternative approach to overcome GC-resistance in leukemia treatment.

Cell Death and Disease (2012) **3,** e349; doi:10.1038/cddis.2012.89; published online 19 July 2012
Subject Category: Cancer

Glucocorticoids (GCs) are common components in chemotherapeutic regimens for lymphoid and myeloid malignancies, including acute lymphoblastic leukemia (ALL), multiple myeloma, chronic lymphocytic leukemia, and non-Hodgkin's lymphoma.[1–3] GCs induce apoptosis regulated by pro- and anti-apoptotic BCL-2 family proteins at the mitochondrial level.[4–7] The BCL-2 family is subdivided into three main groups based on regions of BCL-2 homology (BH) and function: multi-domain anti-apoptotic (e.g., BCL-2, MCL-1, and BCL-X_L), multi-domain pro-apoptotic (e.g., BAX and BAK), and BH3-only pro-apoptotic (e.g. BAD, BID, BIM (BCL-2-interacting mediator of cell death), and PUMA). BH3-only proteins cause cytochrome-*c* release by activating BAX and/or BAK, whereas the anti-apoptotic BCL-2 family of proteins prevents this process.[8,9] We and others have shown that BIM, a pro-apoptotic BH3-only protein, is upregulated by dexamethasone (Dex) treatment in ALL cells and has an essential role in Dex-induced apoptosis.[10,11] BIM could be a prognostic marker for GC response in pediatric ALL.[12] However, the molecular mechanisms of BIM regulation by Dex treatment remain unclear. Accumulating evidence indicates that various external stimuli regulate BIM at several different levels: mRNA transcription, mRNA stability, and posttranslation, for example, phosphorylation. In the context of transcriptional regulation, transcription factors, such as FOXO3a, c-Jun, E2F1, and RUNX1/3, have been reported to regulate *Bim*.[13–20] Furthermore, it has been recently demonstrated that the status of histone acetylation at the *Bim* locus regulates *Bim* expression.[21] *Bim* mRNA stability is controlled by cytokine-regulated Hsc70, which binds to AU-rich elements in the 3′-untranslated region.[22] At posttranslational regulation, extracellular signal-regulated kinase (ERK)-mediated phosphorylation and ubiquitination of BIM can regulate its protein level.[23] Inhibition of phosphorylation by MEK/ERK inhibitors enhances pro-apoptotic activity of BIM by blocking proteasome-dependent degradation. The diverse regulatory mechanisms suggest that the function of BIM can be regulated in different ways in certain situations and that the relative importance of the mechanisms may differ between cell types and external stimuli.

We have previously demonstrated that Dex-induced apoptosis is critically dependent on upregulation of BIM, which is primarily regulated at the mRNA level and also dependent on p38-mitogen-activated protein kinase (MAPK) activation.[24] However, Dex-induced *Bim* upregulation does not seem to be the direct result of transcriptional activity of the GC

[1]Department of Internal Medicine, School of Medicine, Massey Cancer Center, Virginia Commonwealth University, Richmond, VA, USA and [2]Department of Oral and Craniofacial Molecular Biology, School of Dentistry, Massey Cancer Center, Virginia Commonwealth University, Richmond, VA, USA
*Corresponding author: H Harada, Massey Cancer Center, Virginia Commonwealth University, 401 College Street, Richmond, VA 23298, USA. Tel: +804 628 0064; Fax: +804 827 1276; E-mail: hharada@vcu.edu
Keywords: acute lymphoblastic leukemia; glucocorticoid; apoptosis; BIM; c-Jun; Runx2
Abbreviations: BIM, BCL-2-interacting mediator of cell death; BH, BCL-2 homology; Runx2, Runt-related transcription factor 2; GC, glucocorticoid; GR, glucocorticoid receptor; Dex, dexamethasone; shRNA, short hairpin RNA; MAPK, mitogen-activated protein kinase; ALL, acute lymphoblastic leukemia; FOXO, forkhead box O; EMSA, electrophoretic mobility shift assay; qPCR, quantitative PCR
Received 25.1.12; revised 05.6.12; accepted 11.6.12; Edited by H-U Simon

receptor (GR), because (1) *Bim* mRNA induction begins ~4 h after Dex treatment. It is well known that only a few minutes are required for activated GR to bind to a simple promoter regulating gene expression. (2) The putative human *Bim* promoter does not contain any GR response elements. Among the potential *Bim* transcription regulators, the proto-oncogene c-Jun has been shown to have a role in GC-induced apoptosis in leukemia cells, although the target genes are not identified.[25]

In the current study, we used human ALL cell lines to study the molecular mechanisms and signaling pathways of Dex-induced BIM. We identified the critical signaling pathway and molecules for GC-induced apoptosis including c-Jun, Runx2, and BIM.

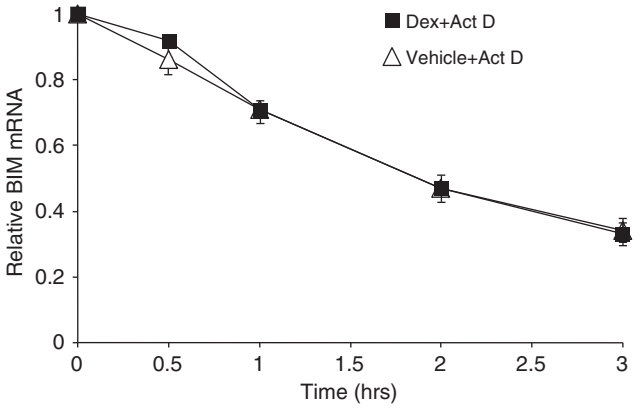

Figure 1 The stability of *Bim* mRNA is not altered by Dex treatment. CEM cells were treated with Dex (0.3 μM) for 16 h followed by actinomycin D (Act D, 1 μg/ml). Cells were harvested at the indicated times and total RNAs were subjected to quantitative PCR (qPCR) to determine the level of *Bim* mRNA. Each level of Dex-treated and -untreated *Bim* mRNA before Act D treatment was considered as 1 and the relative levels were calculated. The results are the mean ± S.D. of triplicates

Results

Dex treatment induces c-Jun and Runx2 expression in ALL cells. In order to study whether the posttranscriptional regulation is involved in Dex-induced *Bim* mRNA levels, CCRF-CEM (CEM) human T-ALL cells were treated with vehicle or Dex for 16 h and then exposed to actinomycin D for various times to inhibit further transcription. The half-life of *Bim* mRNA was identical in control and Dex-treated cells (both for ~1.5 h) (Figure 1), although the absolute level of *Bim* mRNA was ~4–5 folds higher in Dex-treated cells (Figure 2a). These data suggest that Dex does not affect the stability of *Bim* mRNA.

We then performed CEM cells-derived microarray analysis to find the transcription factors in which the expression was significantly changed with Dex treatment. Among several transcription factors in which the expression was up- or downregulated by Dex (Table 1), we focused on c-Jun and Runx2 and validated their regulatory roles on *Bim* transcription. Of note, the expression of Runx1 and Runx3 was not altered by Dex treatment (data not shown). We first examined the expression of c-Jun, Runx2, and BIM in CEM cells before the onset of apoptosis, which begins at 24 h after Dex treatment in this cell line. The levels of *c-Jun* (1.73 ± 0.04 fold) and *Runx2* (1.46 ± 0.22 fold) mRNA started to increase at 30 min after the treatment when *Bim* (1.0 ± 0.08 fold) mRNA expression was still unchanged. *Bim* mRNA started to increase 2 h after the

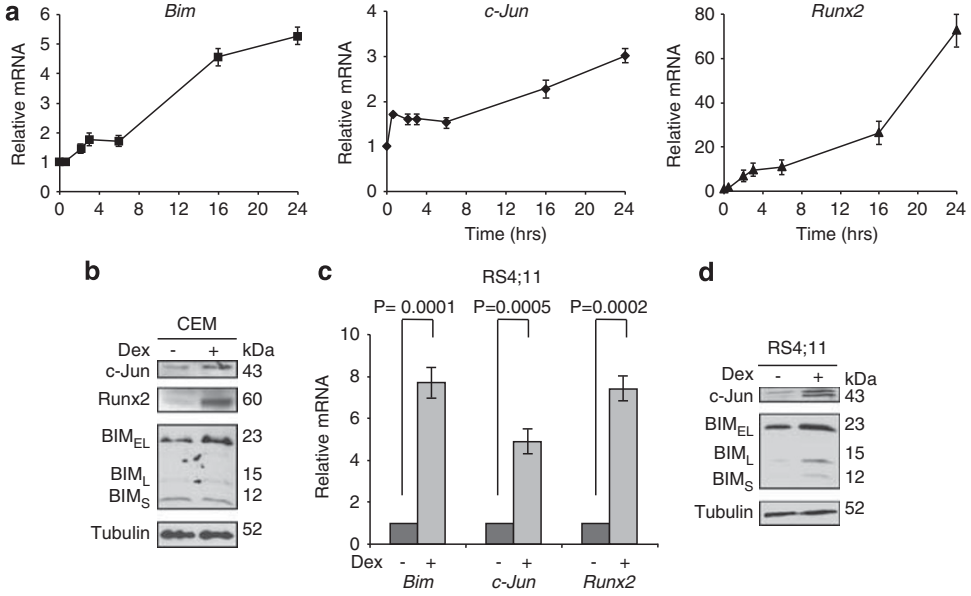

Figure 2 BIM, c-Jun, and Runx2 are induced by Dex in CCRF-CEM (T-ALL) and RS4;11 (B-ALL) cells. (**a**) CEM cells were treated with 0.3 μM Dex for 0.5, 2, 3, 6, 16, and 24 h and total RNAs were subjected to qPCR to determine the levels of *Bim*, *c-Jun* and *Runx2* mRNA. Values represent the mean ± S.D. of three independent experiments. (**b**) CEM cells were treated with 0.3 μM Dex for 24 h and equal amounts of total cell extracts were subjected to western blotting with the indicated antibodies. (**c** and **d**) RS4;11 cells were treated with 0.3 μM Dex for 24 h. Relative *Bim*, *c-Jun*, and *Runx2* mRNAs were determined by qPCR (**c**) and equal amounts of total cell extracts were subjected to western blotting with the indicated antibodies (**d**)

treatment and all three mRNAs continued to increase up to 16–24 h (Figure 2a). At 24 h after Dex treatment, c-Jun, Runx2 and BIM proteins were also accumulated (Figure 2b). We examined another Dex-sensitive ALL cell line RS4;11 and found that the mRNAs and proteins of c-Jun, Runx2, and BIM were induced with Dex treatment (Figures 2c and d). In contrast, either *c-Jun, Runx2,* or *Bim* mRNAs were unchanged with Dex treatment in a Dex-resistant ALL cell line Jurkat (Supplementary Figure S1). These results suggest that c-Jun and Runx2 induction may be prerequisite for BIM induction by Dex treatment.

c-Jun and Runx2 have a pivotal role in BIM expression and cell death induced by Dex. To evaluate the significance of c-Jun in BIM induction and cell death induced by Dex treatment, we established the CEM clones that express dominant-negative c-Jun (TAM67).[26,27] These cells exhibited decreased BIM induction, as well as cell death, induced by Dex compared with the empty vector control cells (Figures 3a and b).

Reciprocally, we generated the CEM clones that overexpress c-Jun cDNA. Both Dex-induced BIM expression and cell death were increased proportionally to the levels of exogenous c-Jun expression; highest in CEM/Jun12 and lowest in CEM/Jun 3 (Figures 3c and d). We confirmed that the amount of Dex-induced *Bim* mRNA was significantly less in the cells harboring dominant-negative c-Jun protein and more in the cells with c-Jun overexpression (Figure 3e). These results indicate that c-Jun has a critical role in *Bim* mRNA induction followed by BIM protein expression and cell death induced by Dex treatment in CEM cells.

Next, we generated CEM cells in which Runx2 was downregulated by short hairpin RNA (shRNA) to examine the significance of Runx2 in BIM induction. Downregulation of Runx2 significantly reduced the mRNA and protein induction of not only BIM but also c-Jun with Dex treatment (Figures 4a and b). As a consequence, Dex-induced cell death was significantly decreased (Figure 4c). The effect of Runx2 shRNA on Dex-induced BIM expression and apoptosis was reversed when c-Jun was overexpressed in CEM/shRunx2 cells (Figures 4d–f). These results strongly suggest that Runx2 is a regulator of Dex-mediated BIM as well as c-Jun induction.

c-Jun but not Runx2 has a direct transcriptional function on the *Bim* promoter. It has been demonstrated that Runx3 is responsible for transcriptional upregulation of *Bim* in

Table 1 Illumina gene array results for CEM cells treated with 0.3 μM Dex for 24 h

Fold change (CEM/Dex *versus* CEM/control)	Regulation (CEM/Dex *versus* CEM/control)	Symbol
49.80916	Up	RUNX2
2.273016	Up	JUN
7.880039	Down	SOX8
7.745545	Down	TFAP2B

Results for transcription factors are shown.

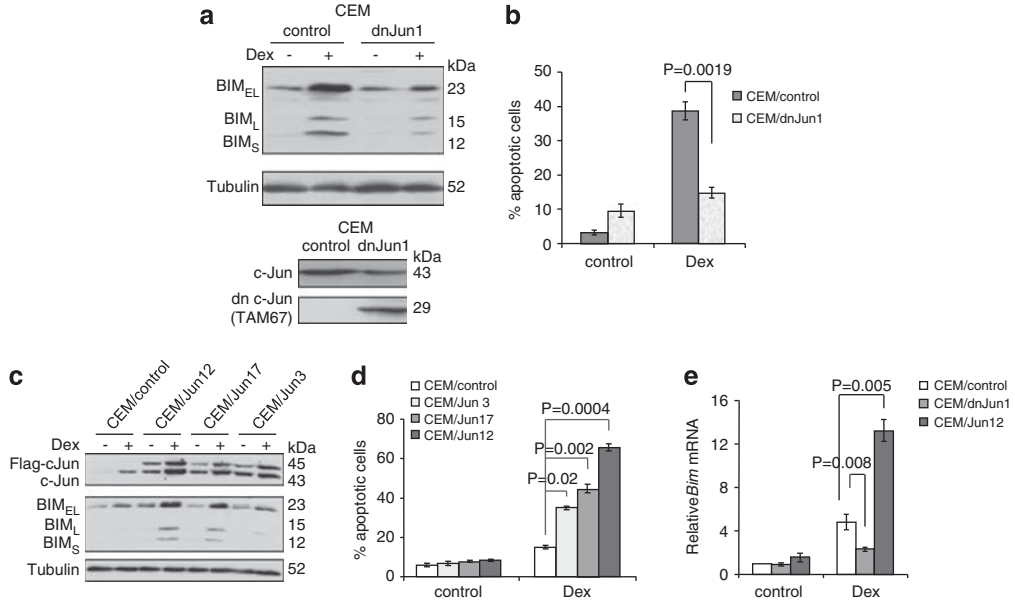

Figure 3 c-Jun regulates BIM expression and cell death induced by Dex. (**a**) A CEM cell clone expressing dominant-negative c-Jun protein (CEM/dnJun1) and control cells (CEM control) were established. Bottom panel shows the expression of a dominant-negative form of c-Jun (TAM67) in CEM/dnJun1 cells analyzed by western blotting with an anti-c-Jun antibody. Cells were treated with 0.3 μM Dex for 24 h and total cell extracts were subjected to western blotting with the indicated antibodies (top panel). (**b**) Cells in (**a**) were treated with 0.3 μM Dex for 48 h and percentage of cell death was determined by AnnexinV-propidium iodide (PI) staining followed by FACS analysis. Values represent the mean ± S.D. of three independent experiments. Another set of each clone yielded equivalent results. (**c**) Three independent CEM clones with overexpression of c-Jun were established. Cells were treated with 0.3 μM Dex for 24 h and total cell extracts were subjected to western blotting with the indicated antibodies. (**d**) Cells in (**c**) were treated with 0.3 μM Dex for 48 h and percentage of cell death was determined by AnnexinV-PI staining followed by FACS analysis. Values represent the mean ± S.D. of three independent experiments. (**e**) CEM/dnJun1, CEM/Jun12, and CEM/control cells were treated with 0.3 μM Dex for 24 h and total RNAs were subjected to qPCR to determine the levels of *Bim* mRNA. Values represent the mean ± S.D. of three independent experiments

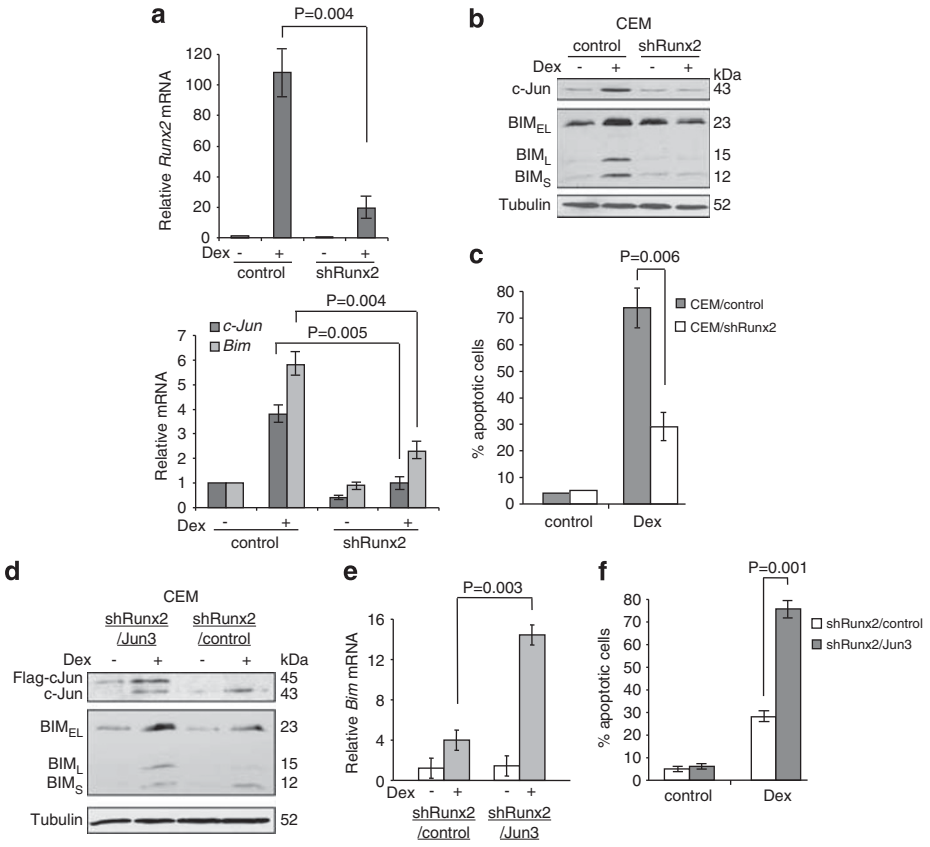

Figure 4 Runx2 regulates BIM expression and cell death induced by Dex. (**a**) CEM cells were infected with lentiviruses expressing shRNAs for non-targeting control or Runx2. Puromycin-resistant cells were pooled after each infection. Cells were treated with 0.3 μM Dex for 24 h and total RNAs were subjected to qPCR to determine the levels of *Bim*, *c-Jun*, and *Runx2* mRNA. (**b**) Cells in (**a**) were treated with 0.3 μM Dex for 24 h and total cell extracts were subjected to western blotting with the indicated antibodies. (**c**) Cells in (**a**) were treated with 0.3 μM Dex for 72 h and percentage of cell death was determined by AnnexinV-PI staining followed by FACS analysis. Values represent the mean ± S.D. of three independent experiments. (**d**) CEM/shRunx2 clone was transfected with Flag-c-Jun cDNA or a vector. The established clones (CEM/shRunx2/Jun3 or CEM/shRunx2/control) were treated with 0.3 μM Dex for 24 h and total cell extracts were subjected to western blotting with the indicated antibodies. (**e**) Cells in (**d**) were treated with 0.3 μM Dex for 24 h and total RNAs were subjected to qPCR to determine the levels of *Bim* mRNA. (**f**) Cells in (**d**) were treated with 0.3 μM Dex for 72 h and percentage of cell death was determined by AnnexinV-PI staining followed by FACS analysis. Values represent the mean ± S.D. of three independent experiments. We analyzed another c-Jun overexpressing clone and the results were reproducible

TGF-β-induced apoptosis in gastric cancer cells.[19] In hepatocyte cells, TGF-β also stimulates *Bim* transcription by upregulating Runx1 expression, which binds FOXO3a, and the two factors cooperate in the transcriptional induction of *Bim*.[20] We searched the c-Jun-binding sites in the human *Bim* promoter and found only one potential AP-1-binding site at about -2.7 kb from the transcription start site (Figure 5a). Interestingly, this binding site is located only $\sim$20 bases apart from the reported Runx-binding site.[19] These binding sites are also found within the conserved region of the mouse *Bim* promoter at about -2.5 kb (data not shown). To examine the function of the putative AP-1- and Runx2-binding sites in the *Bim* promoter in the context of c-Jun and/or Runx 2 expression, a plasmid containing the putative *Bim* AP-1 site upstream of a luciferase reporter gene (*Bim*-luc) was cotransfected with c-Jun and/or Runx2 in 293T cells. Cotransfection with c-Jun activated the *Bim* promoter, but this activation was not augmented by cotransfection with Runx2 (Figure 5b). c-Jun-mediated activation was not observed when the binding sites were deleted in the *Bim*-luc reporter (-1.2 kb). We next generated heterologous *Bim* promoter-luciferase reporter constructs containing intact AP-1- and Runx-binding sites, as well as a mutated AP-1- or Runx-binding site. These reporter constructs were cotransfected with the c-Jun or Runx2 expression vector in 293T cells to examine the function of each binding site on the *Bim* promoter (Figure 5c). The construct containing the intact AP-1- and Runx-binding sites was activated with c-Jun but not Runx2 expression. The AP-1 mutant lost not only the basal level but also c-Jun-mediated activation of the *Bim* promoter. In contrast, the reporter gene harboring a Runx mutation behaved similarly to that harboring the intact sequence. To validate the importance of the AP-1-binding site in the context of Dex treatment, the *Bim* reporter constructs were cotransfected with c-Jun in CEM cells. The activity of the *Bim* reporter was increased after Dex treatment and it was further enhanced by c-Jun cotransfection. (Figure 5d, left). The AP-1 mutant activity was decreased not only at the basal level but also with Dex treatment (Figure 5d, right). These results suggest that c-Jun directly binds and activates the *Bim* promoter, but Runx2 induction by Dex treatment indirectly affects *Bim* promoter activity.

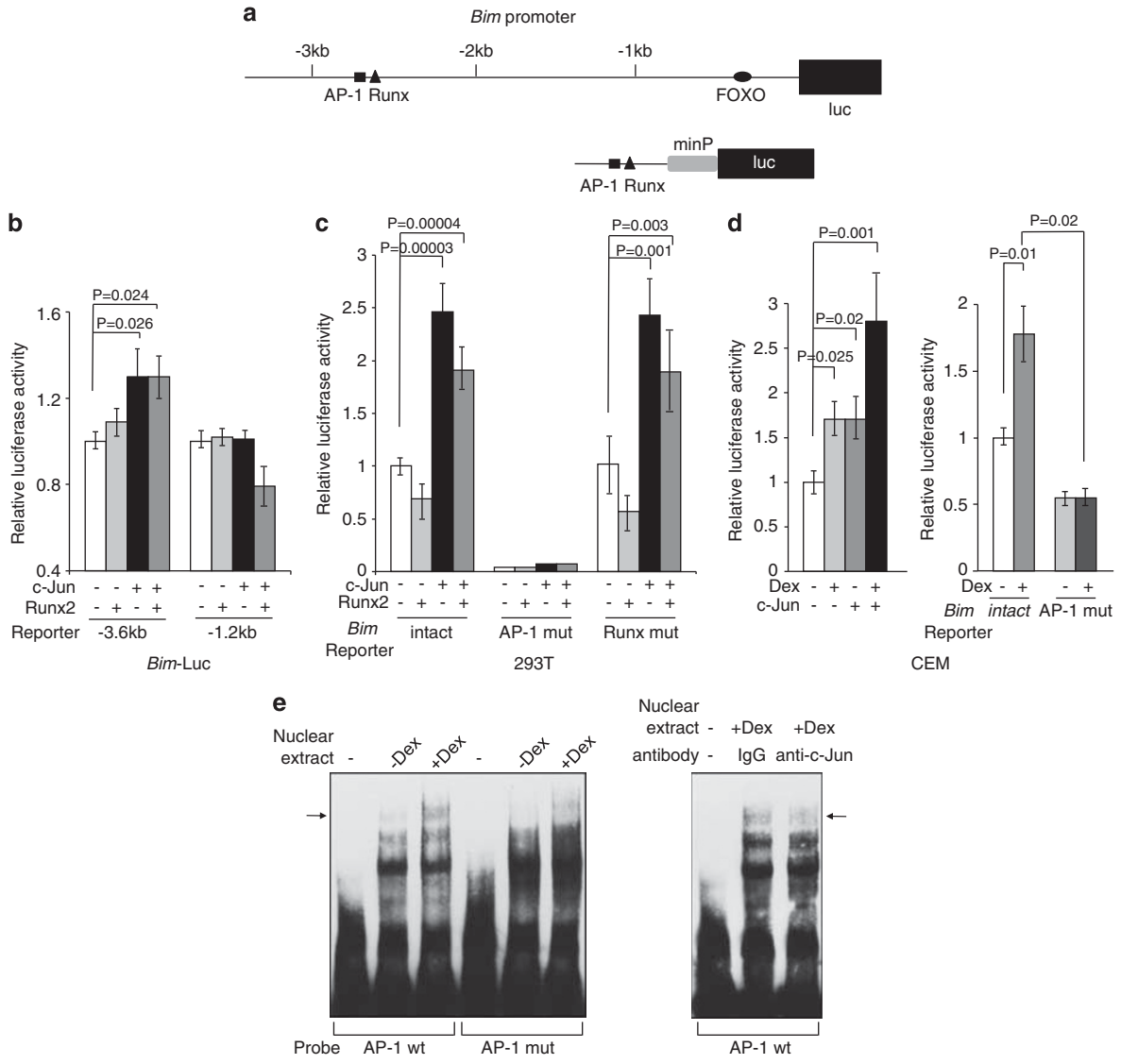

Figure 5 c-Jun binds to and activates the *Bim* promoter. (**a**) Human *Bim* promoter upstream of the start site of transcription contains a Runx-, AP-1-, and FOXO-binding sites. (**b**) The luciferase constructs indicated were cotransfected with a c-Jun and/or a Runx2 expression vectors into 293T cells for 48 h. Luciferase activity was normalized to *Renilla* activity for each well to control for transfection efficiency. Values represent the mean ± S.D. of three independent experiments. (**c**) A luciferase reporter construct containing an intact *Bim* AP-1 and Runx site (*Bim* intact), a mutated AP-1 site (*Bim* AP-1 mut), or a mutated Runx site (*Bim* Runx mut) was cotransfected with a c-Jun and/or a Runx2 expression vectors into 293T cells for 48 h. Luciferase activities were determined as (**b**). Values represent the mean ± S.D. of three independent experiments. minP: minimal promoter. (**d**) The same plasmids in (**c**) were cotransfected into CEM cells. Twenty-four hours after transfection, cells were split into half and continued in culture for another 24 h in the presence or absence of 0.3 μM Dex. Luciferase activities were determined as (**b**). Values represent the mean ± S.D. of three independent experiments. (**e**) Direct binding of c-Jun on the AP-1 site of human *Bim* promoter. Left panel: a probe containing the intact AP-1 site (AP-1 wt) or a probe with mutated AP-1 site (AP-1 mut) was incubated with the nuclear extracts from CEM cells treated in the presence or absence of 0.3 μM Dex for 24 h. An arrow indicates a specific DNA–protein complex. Right panel: anti-c-Jun antibodies were incubated in the reaction mixture. An arrow indicates a probe DNA–c-Jun complex

We confirmed the binding of c-Jun to the putative AP-1 site by an electrophoretic mobility shift assay (EMSA). A DNA–protein complex was detected with a probe containing the intact *Bim* AP-1 site, but not with a mutated AP-1 site probe (Figure 5e, left). The amount of this complex was increased with Dex-treated nuclear extract when total c-Jun expression was increased (Figure 2b). The decrease of the DNA–protein complex by the addition of c-Jun-specific antibody to the reaction mixture confirmed that c-Jun was present (Figure 5e, right). These data indicate that the *Bim* promoter contains a functional c-Jun-binding site in the context of Dex induction.

GR is required for Dex-mediated BIM, Runx2, and c-Jun induction and the induction is regulated by the p38-MAPK pathway. We next addressed the signaling pathways for the induction of BIM, c-Jun, and Runx2. We treated CEM cells with RU486, a GR antagonist, to examine whether RU486 could block c-Jun, Runx2, and BIM induction, as well as apoptosis induced by Dex. Co-treatment with Dex (0.3 μM) and an excess of RU486 (1 μM) inhibited c-Jun, Runx2, and BIM induction, as well as apoptosis to the basal levels (Figures 6a–c), suggesting that all the Dex-mediated induction initiates through GR.

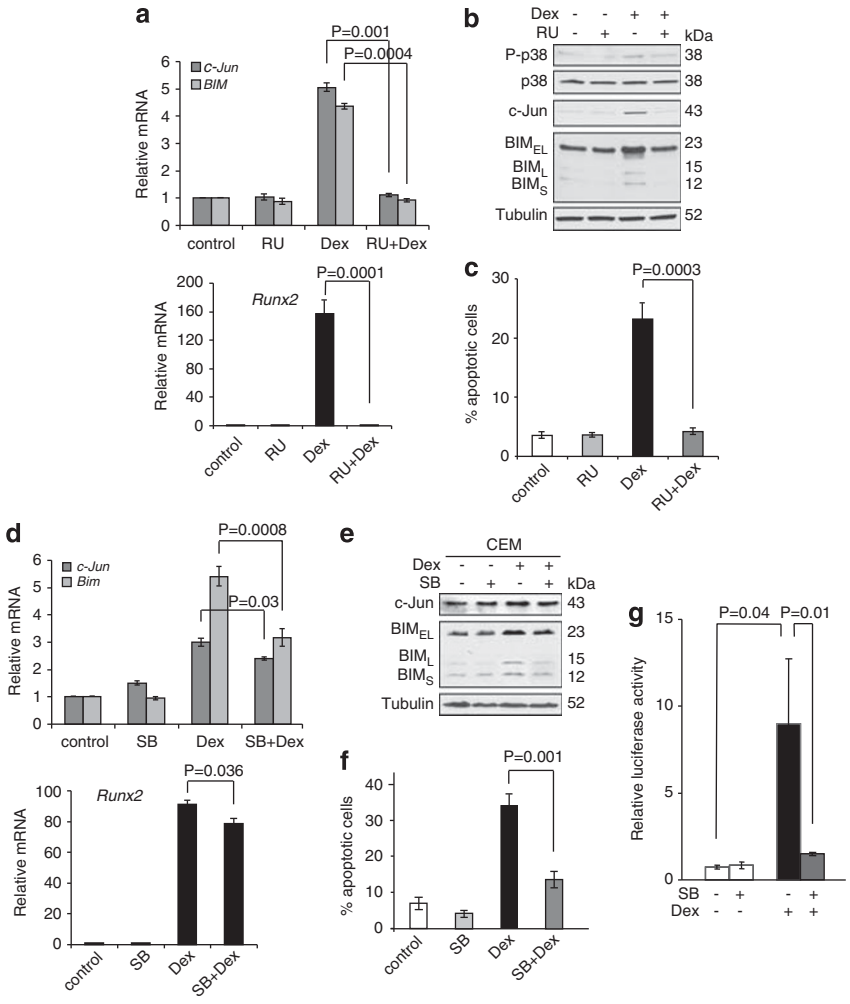

Figure 6 BIM, c-Jun, and Runx2 expression induced by Dex is mediated through the GC receptor-p38-MAPK pathway. (**a**) CEM cells were pretreated with 1 μM RU486 for 30 min and were treated with 0.3 μM Dex for 24 h. Total RNAs were subjected to qPCR to determine the levels of *c-Jun, Runx2,* and *Bim* mRNA. Values represent the mean ± S.D. of three independent experiments. (**b**) CEM cells were treated as (**a**), and equal amounts of total cell extracts were subjected to western blotting with the indicated antibodies. (**c**) CEM cells were treated as (**a**) except Dex treatment was performed for 48 h, and percentage of cell death was determined by AnnexinV-PI staining followed by FACS analysis. Values represent the mean ± S.D. of three independent experiments. (**d**) CEM cells were pretreated with 2 μM SB203580 for 1 h and were treated with 0.3 μM Dex for 24 h. Total RNAs were subjected to qPCR to determine the levels of *c-Jun, Runx2,* and *Bim* mRNA. Values represent the mean ± S.D. of three independent experiments. (**e**) CEM cells were treated as (**d**), and equal amounts of total cell extracts were subjected to western blotting with the indicated antibodies. (**f**) CEM cells were treated as (**d**) except Dex treatment was performed for 48 h, and percentage of cell death was determined by AnnexinV-PI staining followed by FACS analysis. Values represent the mean ± S.D. of three independent experiments. (**g**) A luciferase reporter construct containing AP-1-binding sites (pAP-1-luc) was transfected into CEM cells. Twenty-four hours after transfection, cells were split into half, pretreated with 2 μM SB203580 for 1 h, and were treated with 0.3 μM Dex for another 24 h. Luciferase activity was normalized to *Renilla* activity for each well to control for transfection efficiency. Values represent the mean ± S.D. of three independent experiments

We have previously shown that p38-MAPK activation followed by BIM induction is critical for Dex-induced apoptosis in CEM cells.[24] Treatment with RU486 also inhibited p38-MAPK activation (Figure 6b). We thus examined whether c-Jun and Runx2 induction was also regulated by p38-MAPK activity. CEM cells were treated with SB203580, a p38-MAPK inhibitor, and the levels of c-Jun and BIM with Dex treatment were determined. As a control, SB203580 inhibited Dex-induced phosphorylation of MAPKAPK-2, a direct substrate of p38-MAPK (data not shown).[24] Pretreatment of CEM cells with SB203580 decreased the amount of Dex-induced c-Jun, Runx2, and BIM compared with those in Dex treatment alone (Figures 6d and e), suggesting that p38-MAPK activation contributes to c-Jun, Runx2, and BIM induction. As a consequence, Dex-induced apoptosis was also inhibited by SB203580 (Figure 6f). In order to clarify whether Dex-induced c-Jun activation is p38-MAPK-dependent, an AP-1 luciferase reporter construct was transfected into CEM cells followed by Dex ± SB203580 treatment. The AP-1 luciferase activity was strongly induced by Dex treatment and the induction was abrogated by p38-MAPK inhibition (Figure 6g). This result suggests that c-Jun induction and activation by Dex is p38-MAPK-dependent. Taken together, the data suggest that p38-MAPK contributes to Dex-induced apoptosis through c-Jun, Runx2, and BIM induction.

The FOXO subfamily of forkhead transcription factors, consisting of FOXO3a, FOXO1, and FOXO4, has been shown to function as tumor suppressors and promote their

growth-suppressive effects by upregulating the expression of cell-cycle inhibitory genes and pro-apoptotic genes, such as *Bim*.[13–15] It has also been shown that FOXO3a activation through the p38-MAPK pathway is involved in arsenite-induced *Bim* transcription.[28] We have demonstrated the involvement of the p38-MAPK pathway in Dex-induced BIM induction and apoptosis.[24] Based on these observations, we examined whether the FOXO proteins were also involved in Dex-induced BIM induction. In CEM cells, the expression of FOXO1 was below detectable by western blot analysis. FOXO3a did not show any significant difference in phosphorylation status and in the amount in the nucleus. In contrast, FOXO4 was dephosphorylated and the amount of FOXO4 in the nucleus was increased after Dex treatment (Supplementary Figures S2a and b), indicating FOXO4 translocation and activation. Furthermore, the translocation of FOXO4 into the nucleus was partially inhibited by a p38-MAPK inhibitor, SB203580 (Supplementary Figure S2b). These observations further prompted us to clarify the role of FOXO4 in Dex-induced BIM expression. We generated CEM cells in which FOXO4 was downregulated by shRNA, however, we did not observe any difference in BIM induction by Dex (Supplementary Figure S2c). The results suggest that although FOXO4 is translocated into the nucleus by Dex induction with a p38-MAPK activation-dependent manner, it may not regulate Dex-induced BIM expression.

Discussion

GCs are integral components in the treatment protocols of ALL, multiple myeloma, and non-Hodgkin's lymphoma owing to their ability to induce apoptosis in these malignant cells. We and others have demonstrated that BIM, a BH3-only pro-apoptotic BCL-2 family protein, is a critical molecule in cell death induced by GCs treatment.[7,11,12,21,24] However, GC-mediated regulation of BIM expression remains incompletely understood. It has been recently demonstrated that GCs repress the expression of miR-17-92, which results in elevated BIM protein expression.[29] Because Dex treatment did not affect the stability of *Bim* mRNA (Figure 1), we focused on transcriptional regulation of Dex-induced *Bim*. Our microarray analysis showed that several transcription factors are up- or downregulated by Dex treatment in CEM cells (Table 1). Among them, we focused on c-Jun and Runx2, because (1) it has been shown the involvement of c-Jun in cell death induced by GCs[25] and (2) Runx1 and Runx3 have been shown to regulate *Bim* transcription induced by TGF-β in hepatocytes and gastric cancer cells, respectively.[19,20] Here, we clearly demonstrate that c-Jun and Runx2 are the regulators of *Bim* transcription induced by Dex in ALL cells. The induction of c-Jun and Runx2 by Dex treatment was detected in not only T-ALL CEM cells but also B-ALL RS4;11 cells, indicating that the regulatory mechanism is common. Expression of dominant-negative c-Jun blocked Dex-induced mRNA and protein expression of BIM as well as apoptosis. Reciprocally, overexpression of c-Jun increased Dex-induced mRNA and protein of BIM and apoptosis. Of note, c-Jun overexpression alone slightly induced BIM mRNA and protein (CEM/Jun12 in Figures 3c and e), and BIM expression and apoptosis were further augmented by Dex treatment, suggesting that c-Jun is required for overall BIM expression. Downregulation of Runx2 also reduced Dex-induced BIM and apoptosis. The AP-1- and Runx-binding sites that are potentially bound by c-Jun and Runx2, respectively, are located at ~ -2.7 kb of the promoter with $\sim$20-bp distance. Interestingly, these potential sites are conserved between human and mouse *Bim* promoters that contain approximately 60% homology up to -3 kb. We demonstrated that the AP-1-binding site could be bound by c-Jun and activated by Dex treatment. In contrast, the Runx-binding site was not activated by overexpression of Runx2 (Figure 5). However, downregulation of Runx2 strongly reduced Dex-induced c-Jun expression (Figure 4). These results suggest that Runx2 is an upstream regulator of c-Jun. AP-1 is known to be a dimeric complex formed by the Jun and Fos family of proteins. However, we could not observe the induction of other Jun and Fos family proteins except c-Jun in our microarray data and western blot analysis (data not shown), suggesting that the protein binding to the *Bim* AP-1 site is a c-Jun homodimer.

Runx2 belongs to the family of Runt-domain transcription factors, which bind to a common partner, CBFβ, to form a core binding factor (CBF) complex and can activate or repress gene transcription. Among the family, Runx2 is well known for its role as a master regulator of bone development. In the context of tumor development, Runx2 functions as pro-oncogenic in leukemia/lymphoma and advanced mammary and prostate cancer.[30] In contrast, it has been demonstrated that TGF-β-induced apoptosis is regulated by Runx1 or Runx3. Recently studies have shown that Runx2 binds to the promoter of BAX and induces BAX expression and apoptosis in response to etoposide or cisplatin treatment.[31,32] In our study, Runx2 is involved in Dex-induced *Bim* expression and apoptosis in ALL cells, probably through c-Jun. Of note, the expression of BAX, BAK, BCL-2, BCL-X_L, and MCL-1 is not altered by Dex treatment in CEM cells,[24] thus BIM is the most important factor in this context.

The family of FOXO transcription factors is known to regulate *Bim* transcription in a variety of stimuli. We found that FOXO4 was translocated and activated by Dex treatment in CEM cells. However, our *FOXO4* gene-knockdown experiment suggests that it does not have a role in *Bim* induction (Supplementary Figure S2). Because Dex treatment makes CEM cells in the G1-phase cell-cycle arrest,[10,33] activation of FOXO4 may contribute to the induction of cell-cycle inhibitory genes.

We explored the connection between Runx2/c-Jun induction and the upstream signaling pathways. GC-induced apoptosis is essentially divided into three stages: (1) an initiation stage, which involves GR activation and GR-mediated gene regulation; (2) a decision stage, which engages pro- and anti-apoptotic BCL-2 family proteins at the mitochondrial level; and (3) an execution stage, which involves caspase and endonuclease activation. Ample evidence indicates that the transcriptional activation and repression activity of the GR is required for GC-induced apoptosis. It has been shown that *c-Jun* induction by Dex is primarily a transcriptional phenomenon in CEM cells.[34] In our study, treatment with RU486, a GR antagonist, prevented all downstream events; that is, Dex-induced

p38-MAPK activation, Runx2, c-Jun and BIM induction, and apoptosis (Figures 6a–c). The results indicate that GC binding to GR is essential to GC-mediated induction of downstream molecules. Furthermore, mRNA and protein induction of Runx2, c-Jun, and BIM were also inhibited by the addition of a p38-MAPK inhibitor (Figures 6d and e). However, this inhibitory effect is significantly imposed on BIM expression and marginally on Runx2 and c-Jun expression. In terms of c-Jun induction, (1) JNK (c-Jun N-terminal kinase) was not activated by Dex treatment, (2) treatment with SP600125, a JNK inhibitor, increased, but did not decrease, Dex-induced apoptosis,[24] and (3) c-Jun phosphorylation status was not changed by Dex treatment (data not shown), suggesting that the JNK pathway does not contribute to Dex-induced c-Jun induction and apoptosis. Taken together, these results suggest the following pathways for BIM induction: (1) dependent on p38-MAPK and Runx2/c-Jun, (2) independent of p38-MAPK but dependent on Runx2/c-Jun, and (3) dependent on p38-MAPK but independent of Runx2/c-Jun. GR-activated and p38-MAPK-activated transcription factors could coordinately regulate Dex-induced BIM expression.

In conclusion, we found a critical signaling pathway for GC-induced apoptosis. Resistance to GC in ALL is often associated with defects in apoptosis machinery, not in GR. Therefore, further understanding of the precise signaling pathways and molecules in between the activation of GR and BIM induction could help to develop new therapeutic strategies to combat GC-resistant leukemia and possibly other hematological malignancies.

Materials and Methods

Cell lines and culture. CCRF-CEM, RS4;11, Jurkat, and 293T cells were purchased from the American Tissue Culture Collection (Manassas, VA, USA). Cells were cultured in RPMI 1640 supplemented with 10% heat-inactivated fetal bovine serum, 1 mM sodium pyruvate, streptomycin, and penicillin G at 37 °C in a humidified, 5% CO_2 incubator.

Chemicals and antibodies. Dex, SB203580, and RU486 were purchased from Sigma (St. Louis, MO, USA). Antibodies were purchased as follows: c-Jun (sc-44 to detect TAM67 and sc-45 for other western blot analyses and EMSA), α-Tubulin, p38-MAPK, and Lamin A/C from Santa Cruz Biotechnology (Santa Cruz, CA, USA), BIM, phospho-p38-MAPK, FOXO3a, phospho-FOXO3a, FOXO4, and phospho-FOXO4 (Ser193) from Cell Signaling Technology (Beverly, MA, USA), and Runx2 from MBL International (Woburn, MA, USA).

Gene expression array. Total RNAs from CEM cells with or without Dex treatment for 24 h were subjected to the expression array analysis using Illumina BeadChip (San Diego, CA, USA). Arrays were prepared based on the manufacturer's instruction and scanned on the Illumina Bead Station bead array scanner. Data were analyzed with GenomeStudio software (Illumina).

Quantitative RT-PCR. Total RNA was extracted by Trizol (Invitrogen, Carlsbad, CA, USA) from CEM. RNA of 1 μg was reverse transcribed by High Capacity cDNA Reverse Transcription Kit (Applied Biosystems, Carlsbad, CA, USA) according to the manufacturer's instructions. Using Taqman Gene Expression Assay probe/primer Hs00277190 for *Bim*, Hs00231692 for *Runx2*, and Hs00197982 for *c-Jun* (Applied Biosystems), cDNAs were amplified in a fluorescence thermocycler (Applied Biosystems 7500HT Fast Real-time PCR system) and were analyzed based on the expression level of GADPH with SDS2.2 software (Applied Biosystems).

Western blot analyses. Whole-cell lysates were prepared with CHAPS (3-[(3-Cholamidopropyl) dimethylammonio]-1-propanesulfonate) lysis buffer (20 mM Tris (pH 7.4), 137 mM NaCl, 1 mM dithiothreitol, 1% CHAPS, a protease inhibitor cocktail, and phosphatase inhibitor cocktails (Sigma)). Equal amounts of proteins were loaded on SDS-PAGE, transferred to a nitrocellulose membrane, and analyzed by immunoblotting.

Plasmid transfection and lentivirus infection. A dominant-negative c-Jun (TAM67) expression plasmid was kindly provided by Steven Grant (Virginia Commonwealth University). Flag-tagged c-Jun and Runx2 expression plasmids were purchased from OriGene (Rockville, MD, USA). Transfection was performed by electroporation using a Bio-Rad electroporator (Hercules, CA, USA). The cells were suspended in RPMI 1640 (4×10^6/400 μl) with 10 μg of DNA and electroporated in 0.4 cm cuvettes at 300 V, 500 μF. G418 (800 μg/ml) selection to establish stable cells began 24 h after electroporation. The lentiviral shRNA-expressing constructs were purchased from Open Biosystems (Huntsville, AL, USA). The constructs were transfected into 293T packaging cells along with the packaging plasmids, and the lentivirus-containing supernatants were used to transduce CEM cells.

Cell viability assay. Cell death was quantified by Annexin-V-FITC (BD Pharmingen, San Diego, CA, USA)-propidium iodide (Sigma) staining according to the manufacturer's protocol, followed by flow cytometric analysis using FACScan (BD Biosciences, San Jose, CA, USA).

Luciferase assay. The following oligonucleotide and its antisense were synthesized for *Bim* intact, 5′-CAAAGGTCTCCTGCTGTTAGCGGTGACTCACATTCCCAGTGATTTAGAAAAACTGTGGTGCCGAGTGAA-3′. The solid or broken underlined sequences indicate the consensus AP-1- or Runx2-binding site, respectively. The *Bim* AP-1 mut or *Bim* Runx mut oligonucleotides were synthesized with substitution from the underlined sequences to TATCTCA or TGTCCT, respectively. *Bim* intact-luc, *Bim* AP-1 mut-luc, and *Bim* Runx mut-luc were constructed by inserting the above oligonucleotides between *Kpn*I and *Hin*dIII sites in pGL4.24 (Promega, Madison, WI, USA). The AP-1 luciferase reporter construct (pAP-1-luc) that contains seven times repeated AP-1-binding sites was purchased from Agilent Technologies (Santa Clara, CA, USA). CEM cells were transfected with 5 μg of reporter plasmids, 2 μg of a c-Jun expression plasmid, a Runx2 expression plasmid or an empty vector, and 1 μg pRL-SV40 *Renilla* luciferase plasmid (Promega) using the same transfection protocol described above. 293T cells were transfected using Lipofectamine2000 (Invitrogen). Luciferase activity was measured using Dual-Luciferase Reporter System (Promega) and normalized to the *Renilla* luciferase activity expressed by pRL-SV40.

EMSA. The following 5′-biotinylated oligonucleotide and its antisense were synthesized for AP-1 wt probe by Integrated DNA Technologies (Coralville, IA, USA), 5′-CAAAGGTCTCCTGCTGTTAGCGGTGACTCACATTCCCAGTG-3′. The AP-1 mut probe was synthesized with substitution from the underlined sequences to TATCTCA. Nuclear extracts from CEM cells in the presence or the absence of 0.3 μM Dex for 24 h were prepared using NE-PER kit (Thermo Scientific, Rockford, IL, USA). The binding reactions were performed using Lightshift Chemiluminescent EMSA kit (Thermo Scientific) with 20 fmol probes, 8 μg of nuclear extracts, and 1 μg of poly(dI-dC) in a 20-μl volume at room temperature for 20 min. The samples were then loaded in 6% polyacrylamide gel in 0.5 X TBE and were transferred to nylon membrane. DNA was cross-linked to the membrane using UV cross-linker (Stratagene, Santa Clara, CA, USA). Membranes were incubated according to the manufacturer's protocol. To confirm the presence of c-Jun in the DNA-protein complex, 4 μg of c-Jun antibody (Santa Cruz Biotechnology, sc-45) was added to the binding reaction and incubated for 30 min on ice.

Statistical analysis. Values represent the means ± S.D. for three separate experiments. The significance of differences between experimental variables was determined using the Student's *t*-test. Values were considered statistically significant at $P < 0.05$.

Conflict of Interest

The authors declare no conflict of interest.

Acknowledgements. We would like to thank Steven Grant (VCU) for providing us the TAM67 expression vector and members in his lab for helpful discussion. Gene expression array was performed at the VCU Nucleic Acids Research Facility, which is supported, in part, by funding from the NIH-NCI Cancer

Center Support Grant (P30 CA016059). This work is supported by NIH R01CA134473 and the William Lawrence and Blanche Hughes Foundation (to HH).

1. Tissing WJ, Meijerink JP, den Boer ML, Pieters R. Molecular determinants of glucocorticoid sensitivity and resistance in acute lymphoblastic leukemia. *Leukemia* 2003; **17**: 17–25.
2. Schmidt S, Rainer J, Ploner C, Presul E, Riml S, Kofler R. Glucocorticoid-induced apoptosis and glucocorticoid resistance: molecular mechanisms and clinical relevance. *Cell Death Differ* 2004; **11**(Suppl 1): S45–S55.
3. Bachmann PS, Gorman R, Papa RA, Bardell JE, Ford J, Kees UR *et al.* Divergent mechanisms of glucocorticoid resistance in experimental models of pediatric acute lymphoblastic leukemia. *Cancer Res* 2007; **67**: 4482–4490.
4. Planey SL, Litwack G. Glucocorticoid-induced apoptosis in lymphocytes. *Biochem Biophys Res Commun* 2000; **279**: 307–312.
5. Distelhorst CW. Recent insights into the mechanism of glucocorticosteroid-induced apoptosis. *Cell Death Differ* 2002; **9**: 6–19.
6. Frankfurt O, Rosen ST. Mechanisms of glucocorticoid-induced apoptosis in hematologic malignancies: updates. *Curr Opin Oncol* 2004; **16**: 553–563.
7. Ploner C, Rainer J, Lobenwein S, Geley S, Kofler R. Repression of the BH3-only molecule PMAIP1/Noxa impairs glucocorticoid sensitivity of acute lymphoblastic leukemia cells. *Apoptosis* 2009; **14**: 821–828.
8. Chipuk JE, Moldoveanu T, Llambi F, Parsons MJ, Green DR. The BCL-2 family reunion. *Mol Cell* 2010; **37**: 299–310.
9. Youle RJ, Strasser A. The BCL-2 protein family: opposing activities that mediate cell death. *Nat Rev Mol Cell Biol* 2008; **9**: 47–59.
10. Rambal AA, Panaguiton ZL, Kramer L, Grant S, Harada H. MEK inhibitors potentiate dexamethasone lethality in acute lymphoblastic leukemia cells through the pro-apoptotic molecule BIM. *Leukemia* 2009; **23**: 1744–1754.
11. Zhao YN, Guo X, Ma ZG, Gu L, Ge J, Li Q. Pro-apoptotic protein BIM in apoptosis of glucocorticoid-sensitive and -resistant acute lymphoblastic leukemia CEM cells. *Med Oncol* 2011; **28**: 1609–1617.
12. Jiang N, Koh GS, Lim JY, Kham SK, Ariffin H, Chew FT *et al.* BIM is a prognostic biomarker for early prednisolone response in pediatric acute lymphoblastic leukemia. *Exp Hematol* 2011; **39**: 321–329.
13. Dijkers PF, Medema RH, Lammers JW, Koenderman L, Coffer PJ. Expression of the pro-apoptotic Bcl-2 family member Bim is regulated by the forkhead transcription factor FKHR-L1. *Curr Biol* 2000; **10**: 1201–1204.
14. Gilley J, Coffer PJ, Ham J. FOXO transcription factors directly activate bim gene expression and promote apoptosis in sympathetic neurons. *J Cell Biol* 2003; **162**: 613–622.
15. Essafi A, Fernandez de Mattos S, Hassen YA, Soeiro I, Mufti GJ, Thomas NS *et al.* Direct transcriptional regulation of Bim by FoxO3a mediates STI571-induced apoptosis in Bcr-Abl-expressing cells. *Oncogene* 2005; **24**: 2317–2329.
16. Whitfield J, Neame SJ, Paquet L, Bernard O, Ham J. Dominant-negative c-Jun promotes neuronal survival by reducing BIM expression and inhibiting mitochondrial cytochrome c release. *Neuron* 2001; **29**: 629–643.
17. Biswas SC, Shi Y, Sproul A, Greene LA. Pro-apoptotic Bim induction in response to nerve growth factor deprivation requires simultaneous activation of three different death signaling pathways. *J Biol Chem* 2007; **282**: 29368–29374.
18. Zhao Y, Tan J, Zhuang L, Jiang X, Liu ET, Yu Q. Inhibitors of histone deacetylases target the Rb-E2F1 pathway for apoptosis induction through activation of proapoptotic protein Bim. *Proc Natl Acad Sci USA* 2005; **102**: 16090–16095.
19. Yano T, Ito K, Fukamachi H, Chi XZ, Wee HJ, Inoue K *et al.* The RUNX3 tumor suppressor upregulates Bim in gastric epithelial cells undergoing transforming growth factor beta-induced apoptosis. *Mol Cell Biol* 2006; **26**: 4474–4488.
20. Wildey GM, Howe PH. Runx1 is a co-activator with FOXO3 to mediate transforming growth factor beta (TGFbeta)-induced Bim transcription in hepatic cells. *J Biol Chem* 2009; **284**: 20227–20239.
21. Bachmann PS, Piazza RG, Janes ME, Wong NC, Davies C, Mogavero A *et al.* Epigenetic silencing of BIM in glucocorticoid poor-responsive pediatric acute lymphoblastic leukemia, and its reversal by histone deacetylase inhibition. *Blood* 2010; **116**: 3013–3022.
22. Matsui H, Asou H, Inaba T. Cytokines direct the regulation of Bim mRNA stability by heat-shock cognate protein 70. *Mol Cell* 2007; **25**: 99–112.
23. Ley R, Ewings KE, Hadfield K, Cook SJ. Regulatory phosphorylation of Bim: sorting out the ERK from the JNK. *Cell Death Differ* 2005; **12**: 1008–1014.
24. Lu J, Quearry B, Harada H. p38-MAP kinase activation followed by BIM induction is essential for glucocorticoid-induced apoptosis in lymphoblastic leukemia cells. *FEBS Lett* 2006; **580**: 3539–3544.
25. Zhou F, Thompson EB. Role of c-jun induction in the glucocorticoid-evoked apoptotic pathway in human leukemic lymphoblasts. *Mol Endocrinol* 1996; **10**: 306–316.
26. Brown PH, Chen TK, Birrer MJ. Mechanism of action of a dominant-negative mutant of c-Jun. *Oncogene* 1994; **9**: 791–799.
27. Freemerman AJ, Turner AJ, Birrer MJ, Szabo E, Valerie K, Grant S. Role of c-jun in human myeloid leukemia cell apoptosis induced by pharmacological inhibitors of protein kinase C. *Mol Pharmacol* 1996; **49**: 788–795.
28. Cai B, Xia Z. p38 MAP kinase mediates arsenite-induced apoptosis through FOXO3a activation and induction of Bim transcription. *Apoptosis* 2008; **13**: 803–810.
29. Molitoris JK, McColl KS, Distelhorst CW. Glucocorticoid-mediated repression of the oncogenic microRNA cluster miR-17 ~ 92 contributes to the induction of Bim and initiation of apoptosis. *Mol Endocrinol* 2011; **25**: 409–420.
30. Blyth K, Vaillant F, Jenkins A, McDonald L, Pringle MA, Huser C *et al.* Runx2 in normal tissues and cancer cells: A developing story. *Blood Cells Mol Dis* 2010; **45**: 117–123.
31. Eliseev RA, Dong YF, Sampson E, Zuscik MJ, Schwarz EM, O'Keefe RJ *et al.* Runx2-mediated activation of the Bax gene increases osteosarcoma cell sensitivity to apoptosis. *Oncogene* 2008; **27**: 3605–3614.
32. Goloudina AR, Tanoue K, Hammann A, Fourmaux E, Le Guezennec X, Bulavin DV *et al.* Wip1 promotes RUNX2-dependent apoptosis in p53-negative tumors and protects normal tissues during treatment with anticancer agents. *Proc Natl Acad Sci USA* 2012; **109**: E68–E75.
33. Ausserlechner MJ, Obexer P, Bock G, Geley S, Kofler R. Cyclin D3 and c-MYC control glucocorticoid-induced cell cycle arrest but not apoptosis in lymphoblastic leukemia cells. *Cell Death Differ* 2004; **11**: 165–174.
34. Zhou F, Medh RD, Zhang W, Ansari NH, Thompson EB. The delayed induction of c-jun in apoptotic human leukemic lymphoblasts is primarily transcriptional. *J Steroid Biochem Mol Biol* 2000; **75**: 91–99.

Supplementary Information accompanies the paper on Cell Death and Disease website (http://www.nature.com/cddis)